NAVAL POSTGRADUATE SCHOOL
Monterey, California

THESIS

Modeling Pulse Transmission in the Monterey Bay using Parabolic Equation Methods

by

Eric Lex Westreich

December 1991

Thesis Advisor: Ching-Sang Chiu
Co-Advisor James H. Miller

Approved for public release; distribution is unlimited.

REPORT DOCUMENTATION PAGE

1a. REPORT SECURITY CLASSIFICATION Unclassified	1b. RESTRICTIVE MARKINGS
2a. SECURITY CLASSIFICATION AUTHORITY	3. DISTRIBUTION/ AVAILABILITY OF REPORT Approved for public release; distribution is unlimited.
2b. DECLASSIFICATION/DOWNGRADING SCHEDULE	
4. PERFORMING ORGANIZATION REPORT NUMBER(S)	5. MONITORING ORGANIZATION REPORT NUMBER(S)
6a. NAME OF PERFORMING ORGANIZATION Naval Postgraduate School 6b. OFFICE SYMBOL *(If Applicable)*	7a. NAME OF MONITORING ORGANIZATION Naval Postgraduate School
6c. ADDRESS *(city, state, and ZIP code)* Monterey, CA 93943-5000	7b. ADDRESS *(city, state, and ZIP code)* Monterey, CA 93943-5000
8a. NAME OF FUNDING/SPONSORING ORGANIZATION 6b. OFFICE SYMBOL *(If Applicable)*	9. PROCUREMENT INSTRUMENT IDENTIFICATION NUMBER
8c. ADDRESS *(city, state, and ZIP code)*	10. SOURCE OF FUNDING NUMBERS PROGRAM ELEMENT NO. / PROJECT NO. / TASK NO. / WORK UNIT ACCESSION NO.

11. TITLE *(Include Security Classification)* MODELING PULSE TRANSMISSION IN THE MONTEREY BAY USING PARABOLIC EQUATION METHODS

12. PERSONAL AUTHOR(S)
Eric L. Westreich

13a. TYPE OF REPORT Master's Thesis	13b. TIME COVERED FROM TO	14. DATE OF REPORT *(year, month,day)* December 1991	15. PAGE COUNT 38

16. SUPPLEMENTARY NOTATION
The views expressed in this thesis are those of the author and do not reflect the official policy or position of the Department of Defense or the U.S. Government.

17. COSATI CODES			18. SUBJECT TERMS *(continue on reverse if necessary and identify by block number)*
FIELD	GROUP	SUBGROUP	Fourier synthesis, time domain, parabolic equation, acoustic tomography

19. ABSTRACT *(Continue on reverse if necessary and identify by block number)*

Acoustic tomography signal transmissions in the Monterey Bay are modelled using the time-domain parabolic equation method of Collins and Westwood (1991). Comparison of the model output with the measured arrival structures obtained in Monterey Bay in 1988 shows that this Fourier synthesis can produce good agreement with data. Furthermore, identification of the measured modal arrivals is possible by decomposing the PE model output into individual normal modes. Modal identification provides for the application of tomography in shallow water.

20. DISTRIBUTION/AVAILABILITY OF ABSTRACT [X] UNCLASSIFIED/UNLIMITED [ ] SAME AS RPT. [ ] DTIC USERS	21. ABSTRACT SECURITY CLASSIFICATION Unclassified
22a. NAME OF RESPONSIBLE INDIVIDUAL Ching-Sang Chiu	22b. TELEPHONE (Include Area Code) (408) 646-3239 22c. OFFICE SYMBOL 35 68Ci

Approved for public release; distribution is unlimited.

Modeling Pulse Transmission in the Monterey Bay using Parabolic Equation Methods

by

Eric Lex Westreich
Lieutenant , United States Navy
M.S., University of California, 1988

Submitted in partial fulfillment of the requirements for
the degree of

MASTER OF SCIENCE IN METEOROLOGY AND PHYSICAL OCEANOGRAPHY

from the

NAVAL POSTGRADUATE SCHOOL
December 1991

Chairman, Department of Oceanography

ABSTRACT

Acoustic tomography signal transmissions in the Monterey Bay is modelled using the time-domain parabolic equation method of Collins and Westwood (1991). Comparison of the model output with the measured arrival structures obtained in Monterey Bay in 1988 shows that this Fourier synthesis can produce good agreement with data. Furthermore, identification of the measured modal arrivals is possible by decomposing the PE model output into individual normal modes. Modal identification provides for the application of tomography in shallow water.

TABLE OF CONTENTS

I. INTRODUCTION 1

II. PRESSURE CALCULATION USING FOURIER SYNTHESIS 6

1. A TIME DOMAIN APPROACH 6
2. DETERMINATION OF THE TRANSFER FUNCTION 7
3. PARABOLIC APPROXIMATION 8

III. MODEL USE 11

1. MODEL INPUT 11
2. COMPARISON OF MODEL OUTPUT WITH DATA 12

IV. NORMAL MODE APPLICATIONS 17

1. MODAL DECOMPOSITION 17
2. MODE IDENTIFICATION 18
3. MODE COUPLING 19

V. CONCLUSIONS 27

REFERENCES 28

INITIAL DISTRIBUTION LIST 30

LIST OF FIGURES

Figure 1. Location of Source (A) and Receivers (B through L-2) for the Monterey Bay Tomography Experiment 3

Figure 2. Three-dimensional section of Monterey Bay with source (A) and Station J locations marked. 4

Figure 3. Station J measured 1.9736 second segment averages vs time received (decimal hours starting on December 14, 1988 PST). Every other 16 segment average is plotted for visual clarity. 5

Figure 4. Frequency domain source function used by the Finite Equation Parabolic Equation (FEPE) Fourier synthesis parabolic equation model for the Monterey Bay Experiment 13

Figure 5. Sound velocity profile obtained from CTD measurements on December 14, 1988 near the source. 13

Figure 6. Magnitude squared model output at Station J using a 15 m horizontal range step and one Padé term 14

Figure 7. Magnitude squared model output at Station J using a 15 m range step and two Padé terms 14

Figure 8. Comparison of magnitude squared model output and measured data for Station J. 15

Figure 9. Magnitude squared model output at Station J using a 25 m range step and two Padé terms 16

Figure 10. Eigenfunctions calculated for Station J. The sound velocity profile is also included 20

Figure 11. The magnitude of the model output pressure at the Station J receiver as a function of time and normal mode number. 21

Figure 12a. The magnitude squared for coefficient am time series as a function of mode number at ranges 42.50 and 45.25 km. 22

Figure 12b. The magnitude squared for coefficient am time series as a function of mode number at ranges 45.75 and 49.25 km. 23

Figure 12c. The magnitude squared for coefficient am time series as a function of mode number at ranges 52.50 and 55.75 km (Station J). 24

Figure 13. Bathymetry from the source to Station J 25

Figure 14. Equivalent-ray angles as a function of mode number and range. 26

ACKNOWLEDGMENTS

Professor Ching-Sang Chiu significantly improved my knowledge of ocean acoustics, and provided outstanding guidance on accomplishing this project. Professor Jim Miller's knowledge of signal processing and steady support were also invaluable. This work could not have been accomplished without the love, support and understanding of my wife Joanna.

I. INTRODUCTION

In December, 1988, phase-encoded acoustic signals were transmitted continuously for four days in the waters off Monterey, California to investigate the feasibility of using tomography for ocean interior and surface monitoring in a coastal environment.[1-4] Sound arrival structures were measured from a source (center frequency of 224 Hz and bandwidth of 16 Hz), located in the deep, 881 m, sound channel to several receivers on the shallow, 100 m, adjacent continental shelf (Fig. 1). The path from the source to the receiver at Station J is shown in Fig. 2. Every 16 received 1.9736 second time periods were coherently averaged. The squared magnitude of every other averaged sequence is displayed as a function of time in Fig. 3, for Station J starting on December 14. Stable arrival structures were observed over the duration of the experiment for this path.

A successful application of tomography depends upon the stability, resolvability and identifiability of the acoustic arrivals. If acoustic ray or mode arrival structures are stable, and the individual arrivals have sufficient signal to noise ratio (SNR) and are resolved in time, then the travel times of the rays or modes can be estimated over the duration of the experiment. It is the nature of the acoustic tomography technique that travel time perturbation time series be calculated as the differences between the measured arrival times and modeled or predicted times of arrivals. It is these time series which are the data for the inverse problem. Therefore, to calculate the perturbation, the identification problem in tomography must be solved where actual acoustic ray or mode arrivals are associated with modeled or predicted arrivals. The arrivals in deep water can be identified using ray theory.[5-7]

Ray tracing techniques had mixed success in modeling the propagation in the shallow water of Monterey Canyon[2], and in the Florida Straits.[8] In both these cases, the number of rays present in shallow water became large enough to prevent the identification of individual rays using a single receiver. In addition, Smith found that acoustic rays were extremely sensitive to the exact bathymetry specification of the Monterey Canyon continental slope.[3]

A full wave approach provides a more realistic model of the transmitted signal in the presence of large bathymetric changes. The parabolic equation method developed by Collins[9-13] was chosen for this purpose due its energy conservation scheme, and its ability to efficiently incorporate higher order terms in its approximation of the Helmholtz equation. The steep continental slope gives rise to higher order terms of significant magnitude, and Collins showed that energy conservation is essential when modeling slopes in excess of ten degrees.[9]

Sound arrival identification is accomplished by the decomposition of the pressure field generated by the PE model into normal modes. Additionally, this process provides increased physical understanding of mode coupling and modal sound transmission. Tomographic inverse methods using normal mode travel times have been formulated within the context discussed by Munk and Wunsch for the ocean interior, and Miller et al. for the surface.[1,4,5]

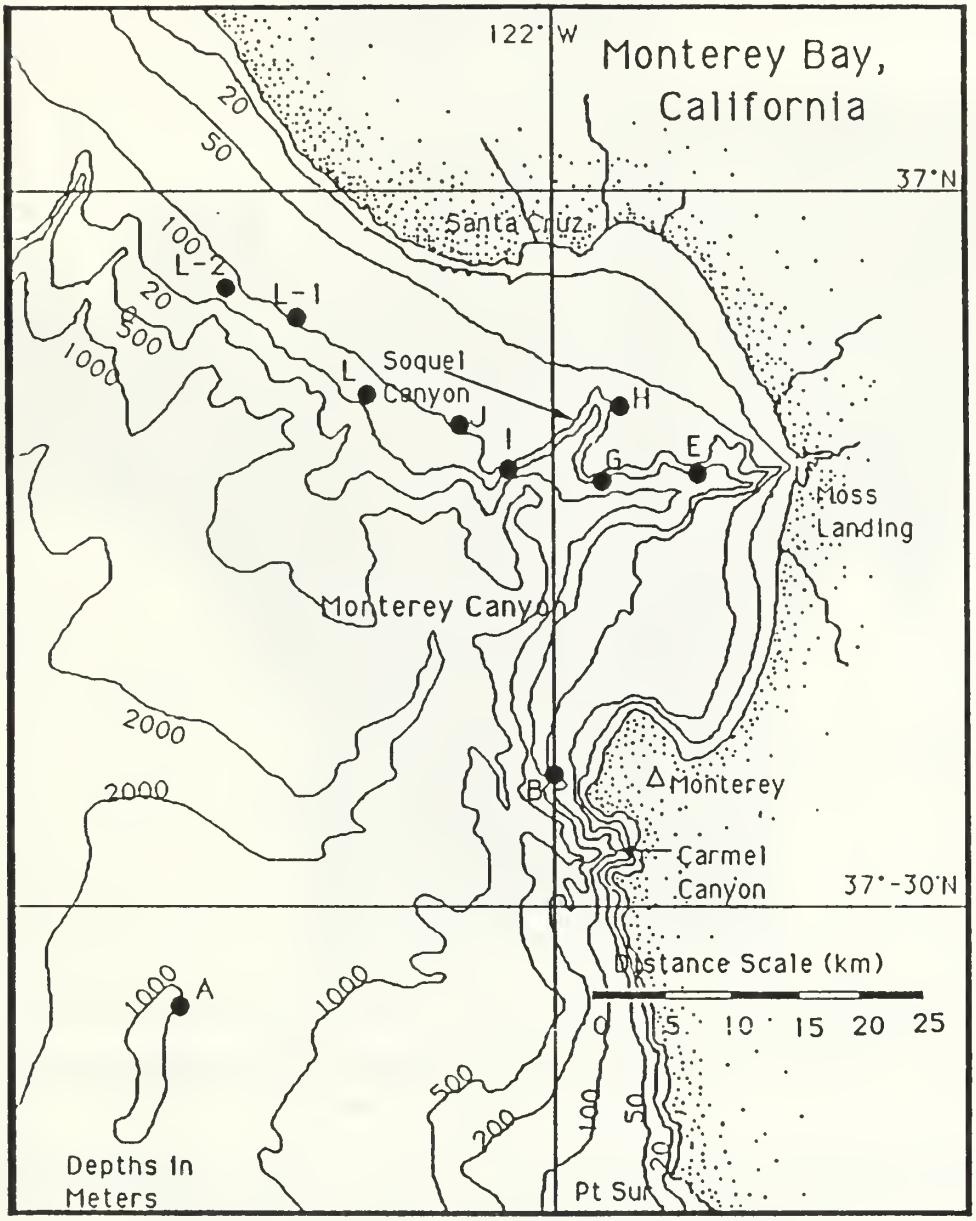

Figure 1. Location of Source (A) and Receivers (B through L-2) for the Monterey Bay Tomography Experiment.

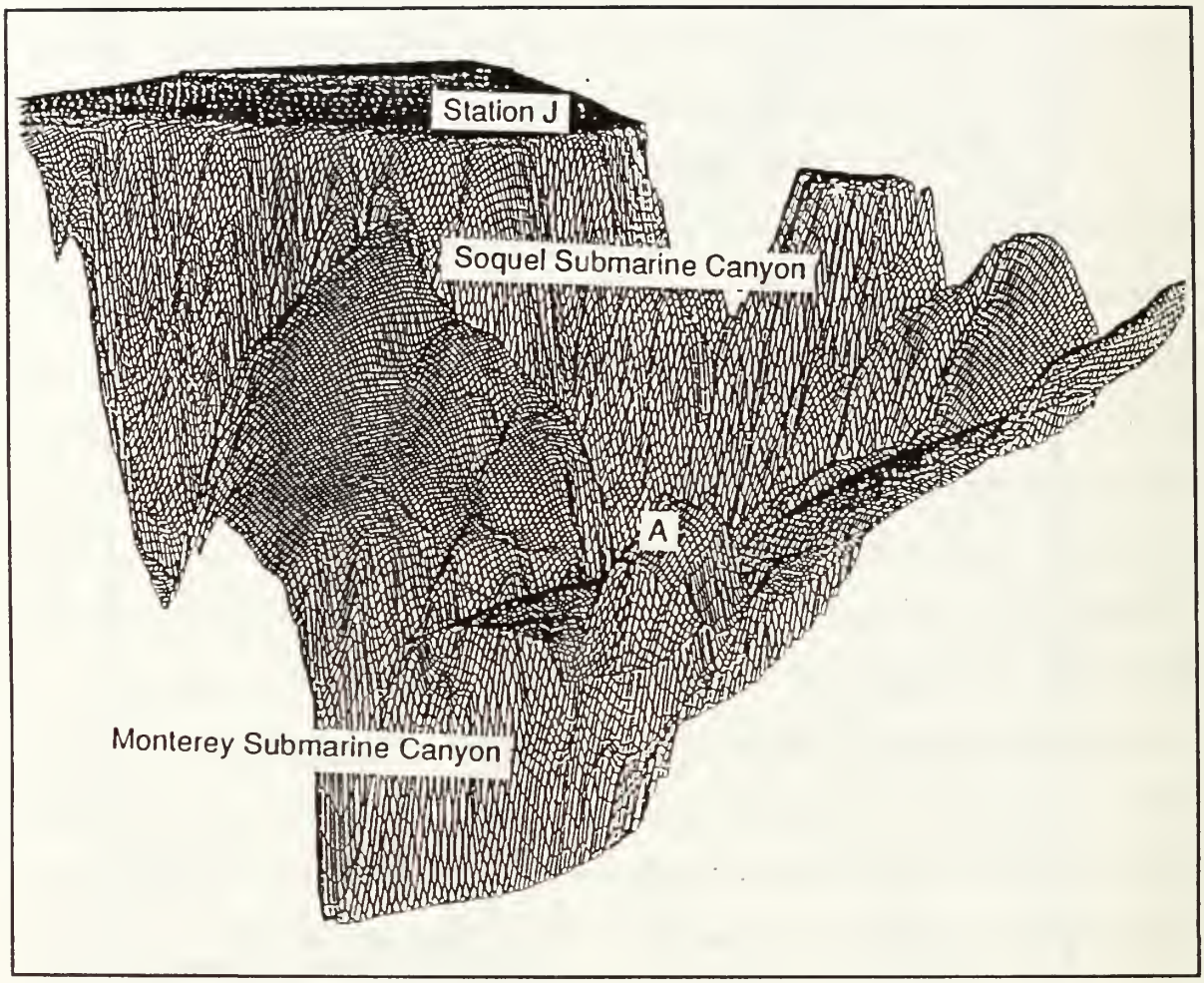

Figure 2. Three-dimensional section of Monterey Bay with source (A) and Station J locations marked.

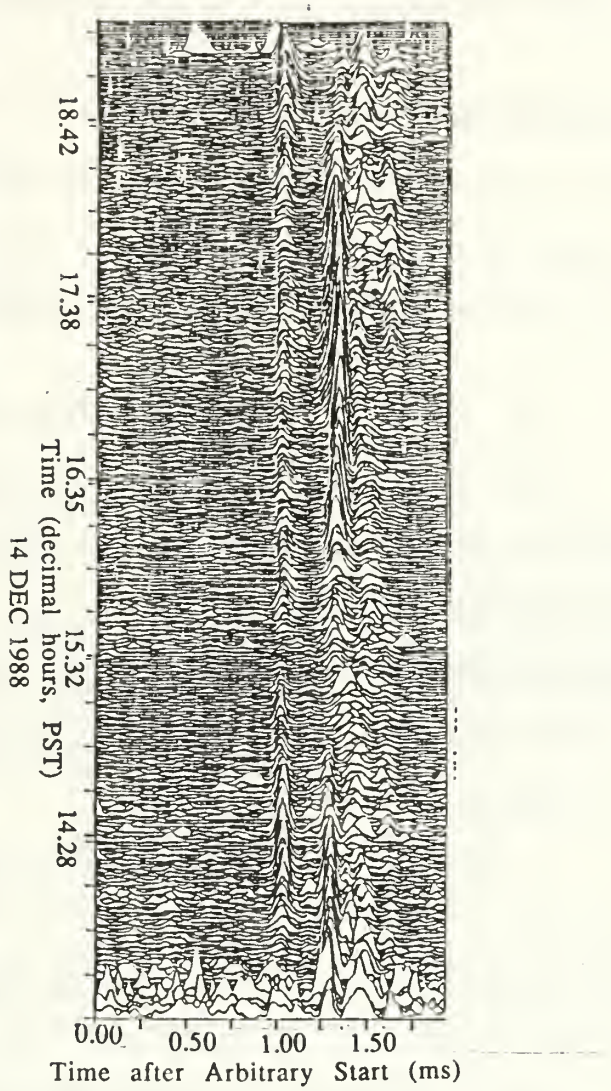

Figure 3. Station J measured 1.9736 second segment averages vs time received (decimal hours starting on December 14, 1988 PST). Every other 16 segment average is plotted for visual clarity.

II. PRESSURE CALCULATION USING FOURIER SYNTHESIS

1. A TIME DOMAIN APPROACH

The receiver time domain pressure signal can be determined, under the assumption of linearity and time invariance, as a convolution of the source pressure and the impulse response of the ocean waveguide:[14]

$$p(r_r, z, t) = \int_{-\infty}^{+\infty} p(r_0, z_0, t-\tau)h(r_0, z_0, r_r, z, \tau)d\tau \qquad (1)$$

where p is pressure, r_0 is the source range, r_r is the receiver range, z_0 is source depth, z_r is receiver depth and t is time.

The Fourier transform of the convolution integral in the time domain is a multiplication in the frequency domain:

$$P(r_r, z, f) = P(r_0, z_0, f) \cdot H(r_0, z_0, r_r, z, f) \qquad (2)$$

Where P and H are the Fourier transforms of p and h respectively such that:

$$p(r_r, z, t) = \int_{-\infty}^{\infty} P(r_r, z, f)e^{-i2\pi ft}df \qquad (3)$$

and

$$h(r_0, z_0, r_r, z, t) = \int_{-\infty}^{\infty} H(r_0, z_0, r_r, z, f) e^{-i2\pi ft} df \qquad (4)$$

Therefore, the pressure in the time domain can also be determined from the inverse Fourier transform of (2):

$$p(r_r, z, t) = \int_{-\infty}^{\infty} P(r_0, z_0, f) H(r_0, z_0, r_r, z, f)\, e^{-i2\pi ft} df \qquad (5)$$

2. DETERMINATION OF THE TRANSFER FUNCTION

The Helmholtz equation governs the sound pressure disturbances excited by a point harmonic source. Therefore, the transfer function can be obtained by solving the Helmholtz equation at different frequencies. Allowing for density variation, the Helmholtz equation is:

$$\rho\nabla\cdot\left(\frac{1}{\rho}\nabla p\right) + k^2 p = -4\pi\delta(\vec{x}-\vec{x}_s) \qquad (6)$$

where k is the wave number, ρ is density, $\vec{x}$ is the position vector, and $\vec{x}_s$ is the spherical point source position vector.[9] Semi-analytical methods such as geometric optics (i.e. ray theory) and separation of variables (i.e. normal modes or fast field), as well as pure numerical schemes such as the parabolic equation methods, can be used. However, as diffraction and dispersion can become important at low frequencies, transfer functions obtained using full wave models, such as normal mode or parabolic equation methods, are better. Normal mode theory is most easily used in ocean environments which are horizontally stratified. Methods exist which account for mode coupling effects resulting from non-horizontal stratification and rough bathymetry.[15,16] However, transfer functions

created using normal mode methods may require significant processing time and storage for deep water regions where many modes are excited. Additionally, separability of the bottom boundary condition can become questionable if rough bathymetry exists.

In the past, the parabolic equation method has been limited to modelling narrow angle sound energy propagation. However, current parabolic acoustic models have been able to model sound with propagation angles close to 90 degrees.[9-13] Furthermore, rough bathymetry and variable stratification are easily implemented. Transfer functions constructed using parabolic approximations are especially suited for low frequency, shallow water, rough bathymetry ocean conditions.

3. PARABOLIC APPROXIMATION

Parabolic equation methods represent the acoustic pressure as the product of two functions:

$$p(r, z) = u(r, z)v(r) \tag{7}$$

where r is the range from the source to the receiver, so that $r = r_r - r_0$. Computation time for a numerical solution is then reduced by expressing rapid variations with range analytically, and leaving the slower variations in range to be determined numerically. The analytic function v(r) changes rapidly with range, while the numerical function, u(r,z), slowly varies in range but can vary rapidly with depth.

Substituting (7) into the Helmholtz equation and neglecting the the backscattered field results in a separable equation for the function v(r) which has an exponential form. Following Collins[11], v(r) is:

$$v(r) = \frac{1}{\sqrt{r}} e^{i k_0 r} \tag{8}$$

Substituting for v(r) and factoring results in a parabolic equation for u(r,z) which includes an unwieldy square root operator:

$$\frac{\partial u}{\partial r} = ik_0\left(\sqrt{1+X} - 1\right)u \tag{9}$$

where

$$X = k_0^{-2}\left(k^2 - k_0^2 + \frac{\partial^2}{\partial z^2} - \frac{1}{r}\frac{\partial r}{\partial z}\frac{\partial}{\partial z}\right)$$

The square root operator has been simplified using either a Taylor series[17], a rational function[18] or a Padé series[9-13] approximation. The Finite Element Parabolic Equation (FEPE) of Collins uses a family of Padé series to create higher order parabolic equations which are accurate for propagation angles close to 90 degrees.[9-13]

Using Padé series, the FEPE approximates the square root operator as:

$$\sqrt{1+X} - 1 = \sum_{j=1}^{n} \frac{a_{j,n} X}{1 + b_{j,n} X}$$

$$a_{j,n} = \frac{2}{2n+1} \sin^2 \frac{j\pi}{2n+1} \tag{10}$$

$$b_{j,n} = \cos^2 \frac{j\pi}{2n+1}$$

The number of Padé terms used determines the angle of sound propagation which can be accurately modelled. While the use of one term is equivalent to the wide angle PE, having an approximately 40 degree propagation angle, the use of four terms provides accuracy of close to 90 degrees depending on the ocean environment. The amount of computer time required increases proportionally with the number of Padé terms used.[9-13]

Substituting the parabolic form for the frequency domain transfer function (Eq. 7), the time domain pressure signal can be evaluated as:

$$p(r_r, z, t) = \int_{-\infty}^{\infty} P(r_0, z_0, f)u(r, z, f)v(r, f)e^{-i2\pi ft}df \qquad (11)$$

Substituting for the chosen value of v(r)

$$p(r_r, z, t) = \int_{-\infty}^{\infty} P(r_0, z_0, f)u(r, z, f)\frac{1}{\sqrt{r}}e^{ik_0 r}\, e^{-i2\pi ft}df \qquad (12)$$

Using the fact that $k_0 = \frac{2\pi f}{c_0}$, and combining exponential terms, (12) becomes:

$$p(r_r, z, t) = \int_{-\infty}^{\infty} P(r_0, z_0, f)u(r, z, f)\frac{1}{\sqrt{r}}\exp\left(-i2\pi f\left(t - \frac{r}{c_0}\right)\right)df \qquad (13)$$

With a change of time variable:

$$t' = t - \frac{r}{c_0}$$

where $\frac{r}{c_0}$ is the reference travel time of a plane wave solution, the resulting pressure is

$$p(r_r, z, t') = \int_{-\infty}^{\infty} P(r_0, z, f)u(r, z, f)\frac{1}{\sqrt{r}}\, e^{-i2\pi ft'}df \qquad (14)$$

The integral expression is solved numerically using the inverse fast Fourier transform (IFFT).

III. MODEL USE

1. MODEL INPUT

Modifications in FEPE_SYN, a prototype Fourier synthesis code developed by Collins[9-13] allowed for its use in modelling the acoustic propagation from the transmitter to Station J in the Monterey Tomography Experiment. The Blackman function was used to represent the transmitting signal in the frequency domain. The center frequency of the function was 224 Hz, the same as the actual source, with the function having zero values below 212 Hz and above 236 Hz to represent the source's ± 12 Hz bandwidth (Fig. 4). The Blackman function provided a sharp but smooth cutoff above and below the bandwidth, reducing the sidelobes in the time domain. The inverse Fourier transform of the Blackman function closely approximated the output of the correlator receiver used in the experiment.

The bathymetry used was obtained from NOAA[19] and had a grid spacing of 250 meters. The SVP used was obtained near the transmitter during the 1988 Monterey Bay Experiment. The small variation between the sound velocity profile measured at the source and the receiver allowed the deep water SVP to be used along the entire sound path (Fig. 5). Bottom sound speed, density and attenuation were taken to be the average values for continental shelf silty sand as obtained by Clay and Medwin.[20]

The sampling interval in the computational example is one millisecond (ms). The resulting Nyquist frequency of 500 Hz, is more than twice the maximum frequency used of 236 Hz. The time window starts 440 ms before the expected

arrival of a plane wave solution, travelling at a speed of c_0, and arriving at time $t = r/c_0$. The arrivals are tracked for 1600 ms after the reference plane wave solution arrival.

2. COMPARISON OF MODEL OUTPUT WITH DATA

The resulting wide angle, one Padé term, computer modelled output accounts for sound energy propagating accurately up to 40 degrees, and shows a series of arrivals starting 140 ms after the plane wave reference (Fig. 6). A large double peaked pulse is shown between two smaller peaks. Taking the higher order terms into account, using two Padé terms, the constructive and destructive interference of the higher order energy is seen as an increase in the amplitude of the predicted signal, and a narrowing of the double peaked pulse to a single peak. The major pulse amplitude is also increased (Fig. 7). The computer output from the higher-order example shows good qualitative agreement with the measured station J data.

The predicted and the measured results show an initial arrival, followed by a narrow, larger pulse quickly followed by a series of smaller amplitude arrivals. The spacing between the pulses and the relative amplitudes of the arrivals, both plotted as amplitude squared in Fig. 8, are in agreement. The excellent agreement of the higher-order model output with the measured data, versus that of the lower order output, demonstrates the importance of including the higher-order terms in modelling the Monterey Bay propagation. Higher-order terms can be important in cases where steep bathymetry exists such as in this example.

Model output shows a sensitivity to the horizontal range step chosen. The reproduction of the measured results, by the time domain model, required the use

of a 15 meter range step. The use of a larger range step produced arrivals of excessive width, as shown in Fig. 9.

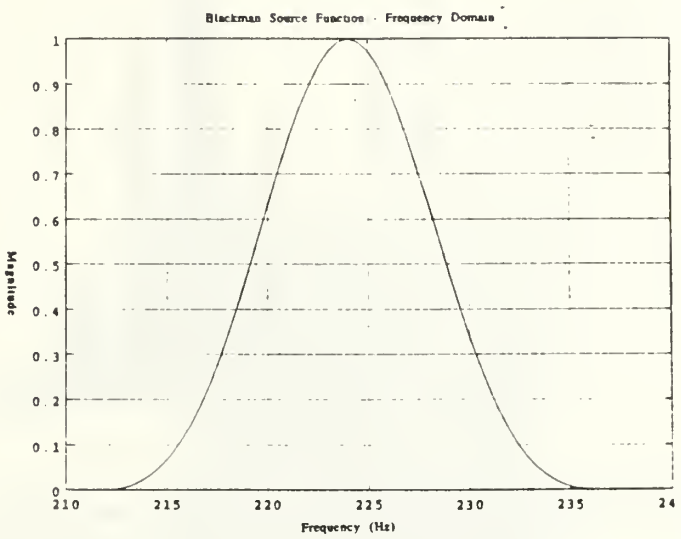

Figure 4. Frequency domain source function used by the Finite Equation Parabolic Equation (FEPE) Fourier synthesis parabolic equation model for the Monterey Bay Experiment.

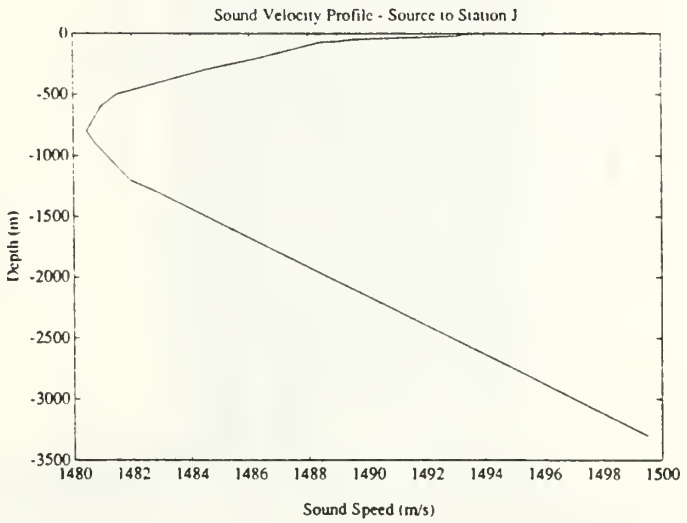

Figure 5. Sound velocity profile obtained from CTD measurements on December 14, 1988 near the source.

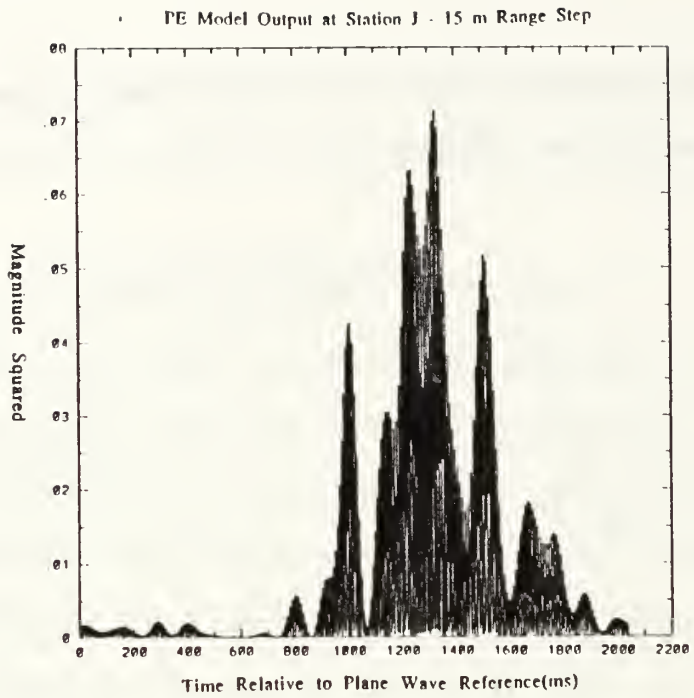

Figure 6. Magnitude squared model output at Station J using a 15 m horizontal range step and one Padé term.

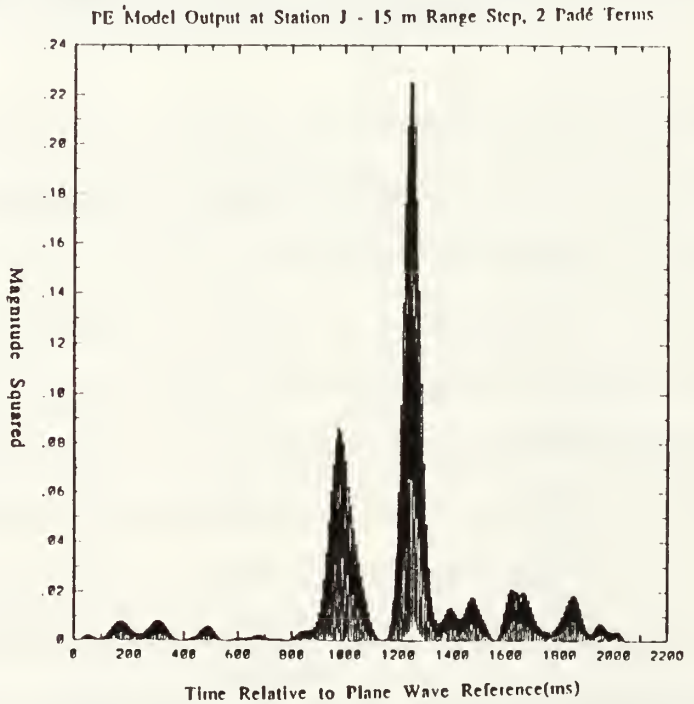

Figure 7. Magnitude squared model output at Station J using a 15 m range step and two Padé terms.

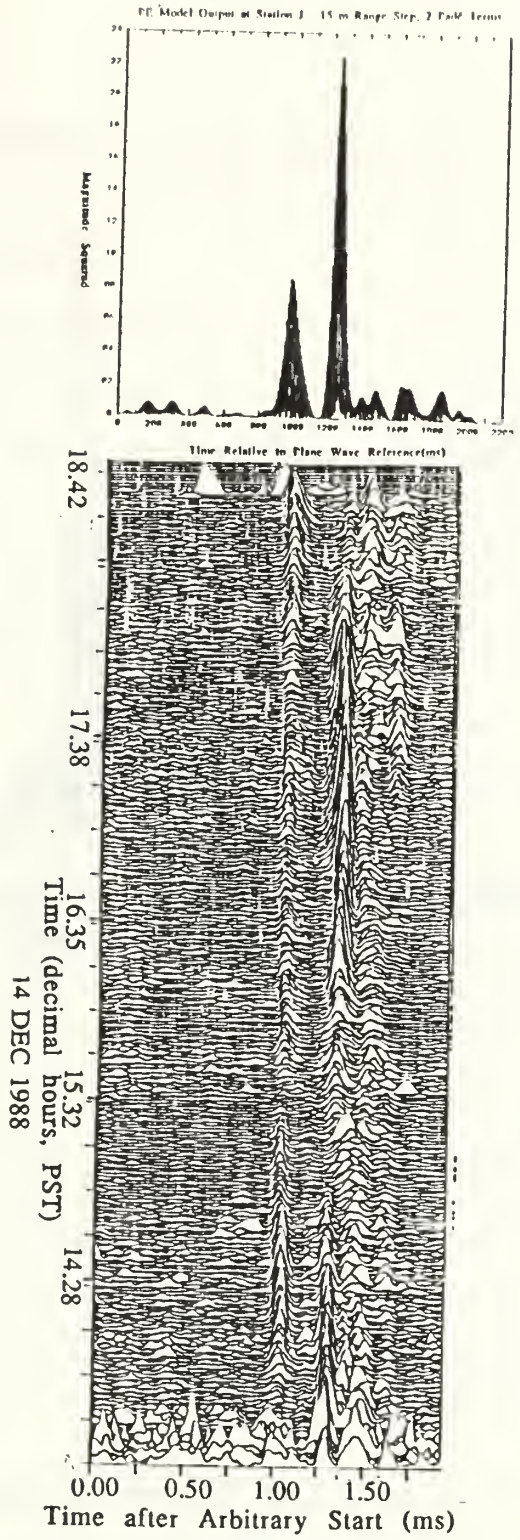

Figure 8. Comparison of magnitude squared model output and measured data for Station J.

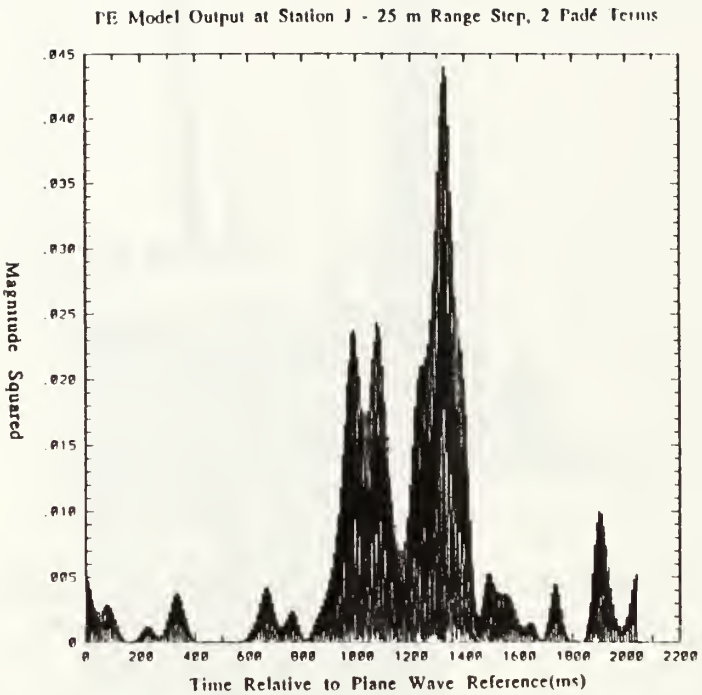

Figure 9. Magnitude squared model output at Station J using a 25 m range step and two Padé terms.

IV. NORMAL MODE APPLICATIONS

1. MODAL DECOMPOSITION

Modal decomposition provides a physically meaningful display of output from the parabolic approximation. In addition, normal mode travel time information can be used for tomographic inversion.[1,4,5] In particular, time domain modal fluctuations can be used to determine the surface frequency spectrum, as verified by surface buoys deployed in the 1988 Monterey Bay Experiment.[1,4]

Sound energy arriving at a receiver can be described as the sum of normal modes (Fig. 10) $Z_m(z)$:

$$p(r, z, t) = \sum_{m=1}^{\infty} a_m(r, t) \cdot Z_m(r, z, t) \tag{15}$$

where p is pressure, a_m is the coefficient, Z_m is the eigenfunction, and m is the mode number. Although there are an infinite number of modes possible, only finite number of modes will be trapped in the ocean wave guide, depending on the frequency, the depth of the channel, the SVP and the boundary conditions.[20] The number of trapped modes at the receiver can be estimated by approximating the coastal shelf area of Station J as an isospeed sound channel bounded by a pressure release surface and a sediment bottom.

Thirteen trapped modes are estimated using the equation:

$$m \leq \frac{f}{c_0}(2h\cos\theta_c) + \frac{1}{2} \tag{16}$$

where m is the number of modes trapped, f is frequency, c_0 is the sound speed in the channel, h is the water column depth.[20] The critical angle, θ_c, is defined by

$$\frac{\sin\theta_c}{c_0} = \frac{1}{c_1} \tag{17}$$

where c_1 is the sediment sound speed.

The modes are computed by solving:

$$\left(\frac{d^2}{dz^2} + k^2 - k_n^2\right) z_m = 0 \tag{18}$$

subject to the boundary conditions. The actual SVP and a finite difference approximation are used.

Since Z_m 's are orthogonal functions, i.e.,

$$\int_0^\infty Z_m(r, z) Z_n(r, z) dz = \delta_{mn}(z) \tag{19}$$

the coefficient a_m's can be obtained by integrating the products of the computed pressure and the normal modes:

$$a_m = \int_0^\infty p(r, z, t) \cdot Z_m(r, z) dz \tag{20}$$

The pressure time series can be seen at the Station J receiver for each mode in Fig. 11.

2. MODE IDENTIFICATION

Acoustic tomography requires that measured sound arrivals be identified with the predicted arrivals. The maximum amplitude measured arrival is coincident with the maximum predicted sound arrival. The sound arrival at station J can be seen in Fig. 11 to be clearly dominated by mode 6 sound energy. The second largest amplitude arrival, which just precedes the largest arrival, is also dominated by mode six. However, modes one, five and eight are also represented. The use of

a hydrophone array instead of a single receiver should make it possible to measure individual modal arrivals.

3. MODE COUPLING

Sound energy can be seen to move from higher to lower modes as sound moves up the slope in Monterey Bay to Station J on the continental shelf, (Fig. 12 and Fig. 13). Relating normal modes to rays facilitates the explanation of this occurrence. In this context, ray behavior can be seen as the constructive interference of neighboring normal modes. Parameterizing mode quantities by mode number and equivalent ray angle allows an "equivalent-ray" to be found such that each resonance is centered at an equivalent-ray angle. These rays are "fuzzy" in that they have finite width, and then a sound beam may be used to represent a ray at a finite frequency.[21,22] The ray incident angles increase as sound travels up the slope due to bottom interactions. Ray equivalent angles of modes also increase as the depth decreases.

Mode energy is concentrated in higher modes at the base of the slope, with mode 18 dominant. The equivalent-ray angle is approximately 2.5 degrees, as shown in Fig. 14. A ray propagating at this angle will interact with the bottom only once on the slope. The bottom interaction will increase the incident angle at the continental shelf to approximately 12 degrees. The mode which has the resulting ray-equivalent angle of 12 degrees is mode six. Therefore, we would expect that mode 6 energy will be dominant as is explained using a ray analogy.

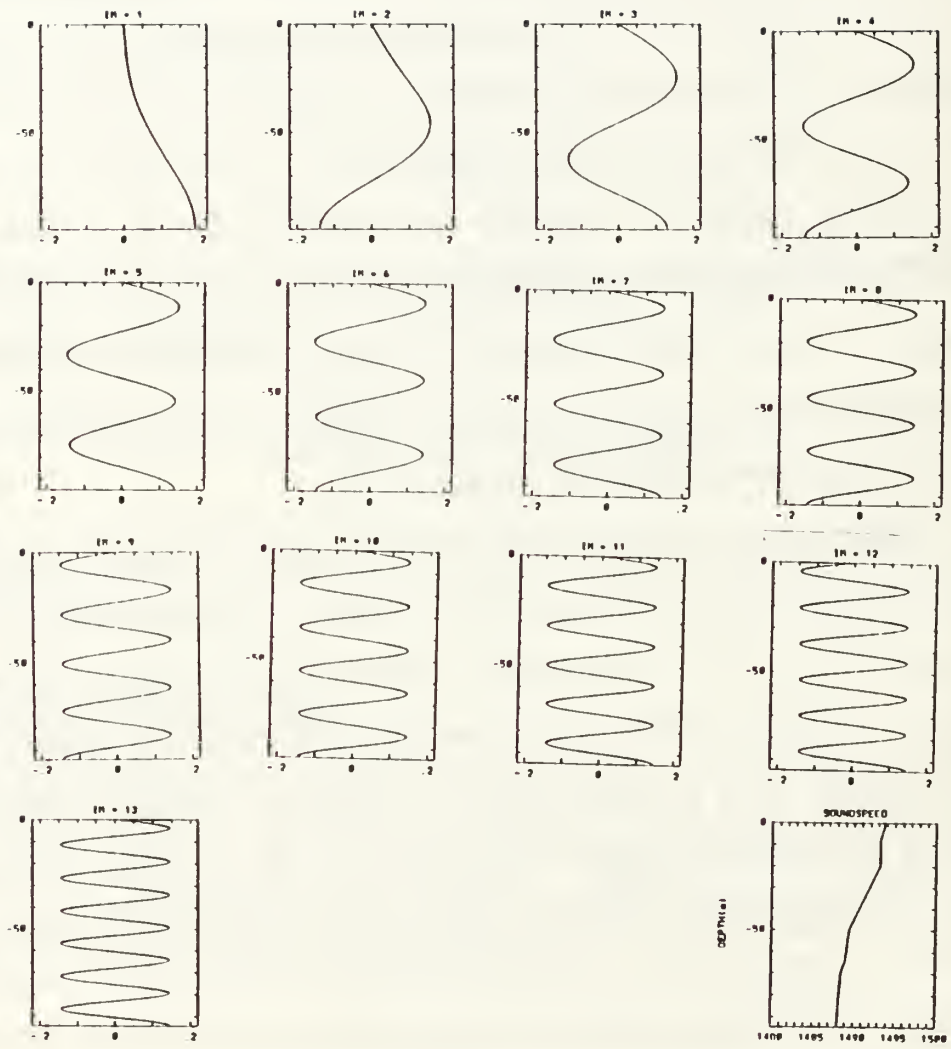

Figure 10. Eigenfunctions calculated for Station J. The sound velocity profile is also included.

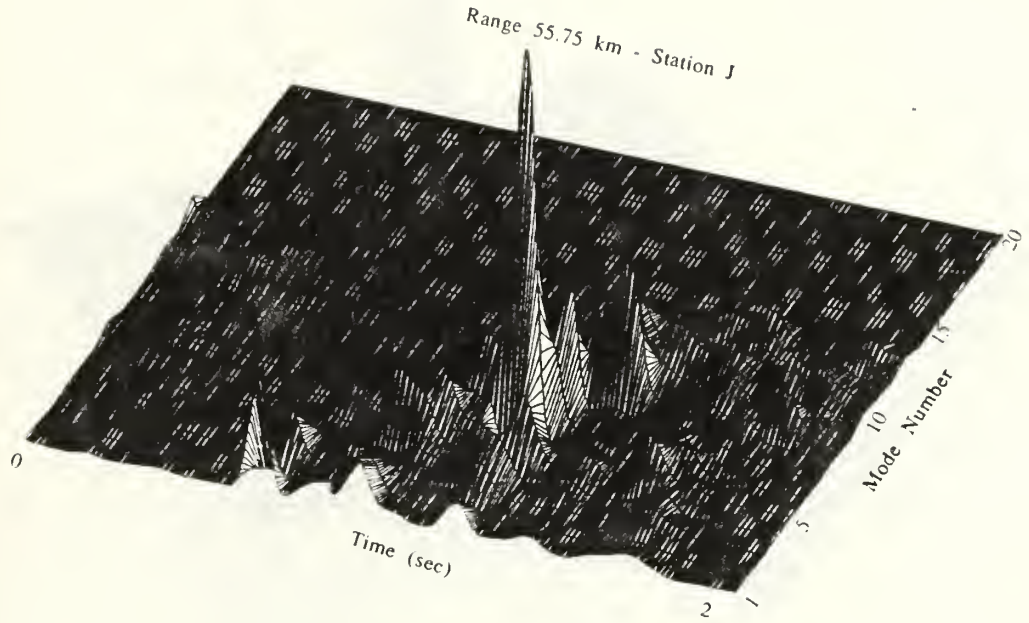

Figure 11. The magnitude of the model output pressure at the Station J receiver as a function of time and normal mode number.

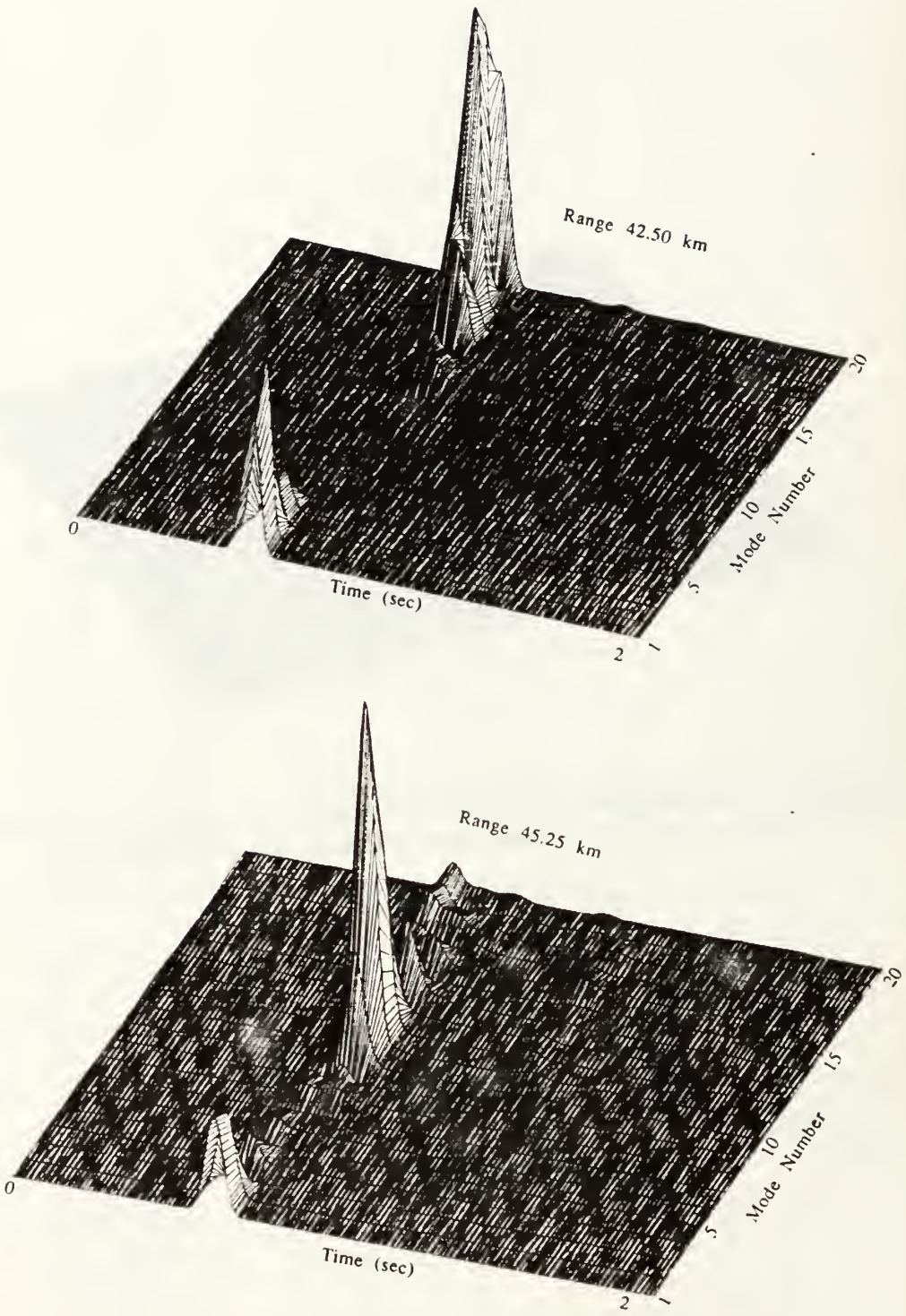

Figure 12a. The magnitude squared for coefficient a_m time series as a function of mode number at ranges 42.50 and 45.25 km.

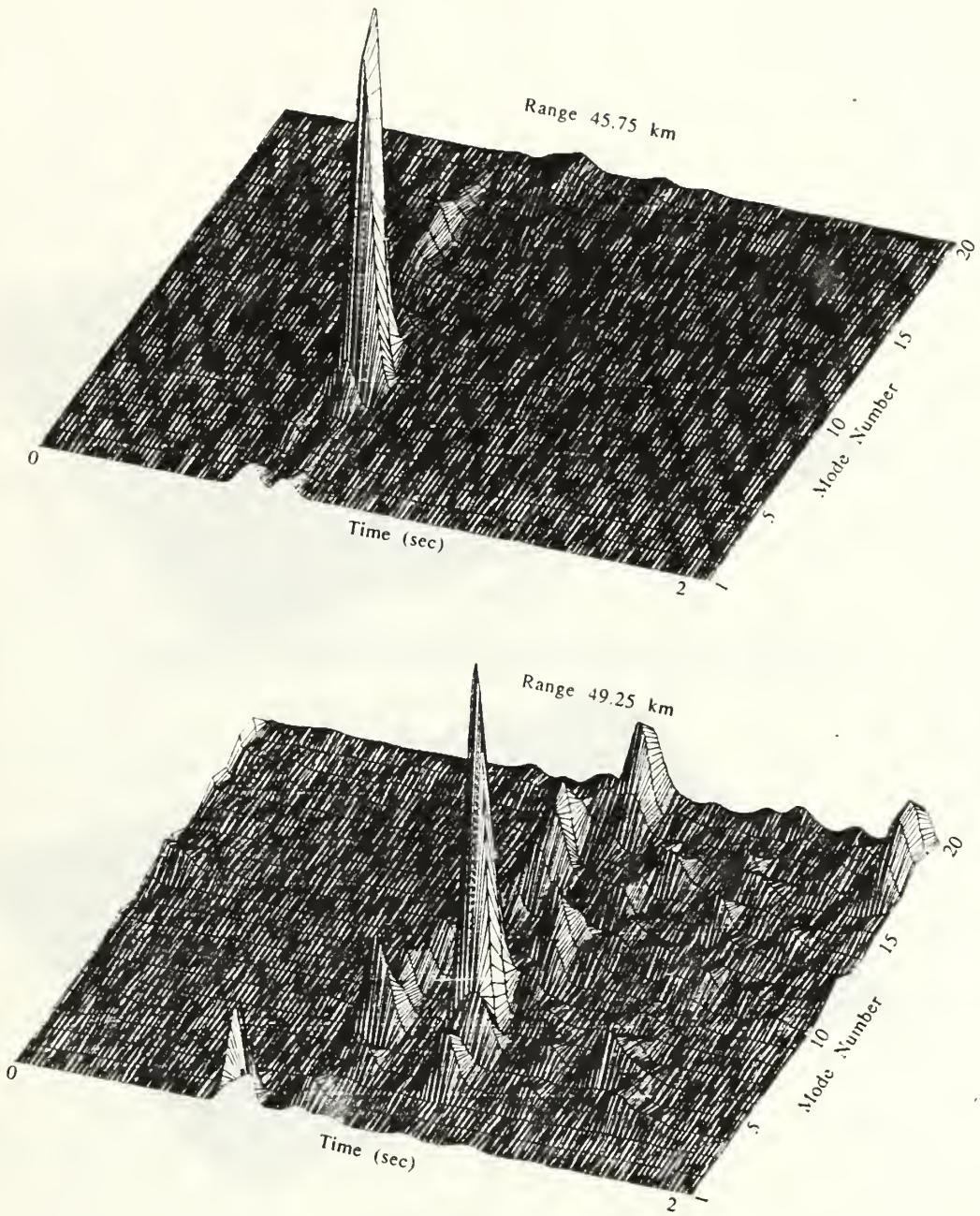

Figure 12b. The magnitude squared for coefficient a_m time series as a function of mode number at ranges 45.75 and 49.25 km.

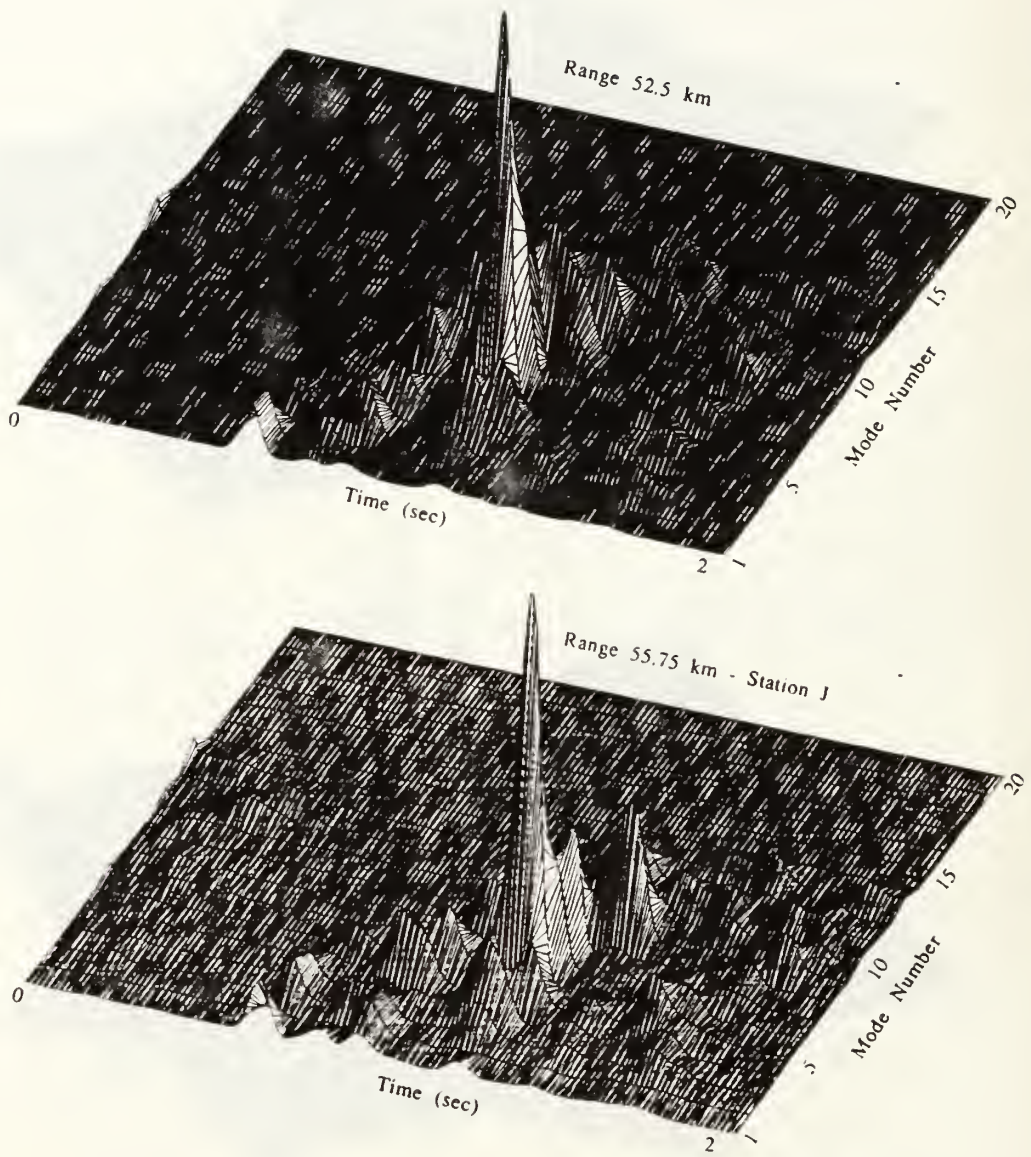

Figure 12c. The magnitude squared for coefficient a_m time series as a function of mode number at ranges 52.50 and 55.75 km (Station J).

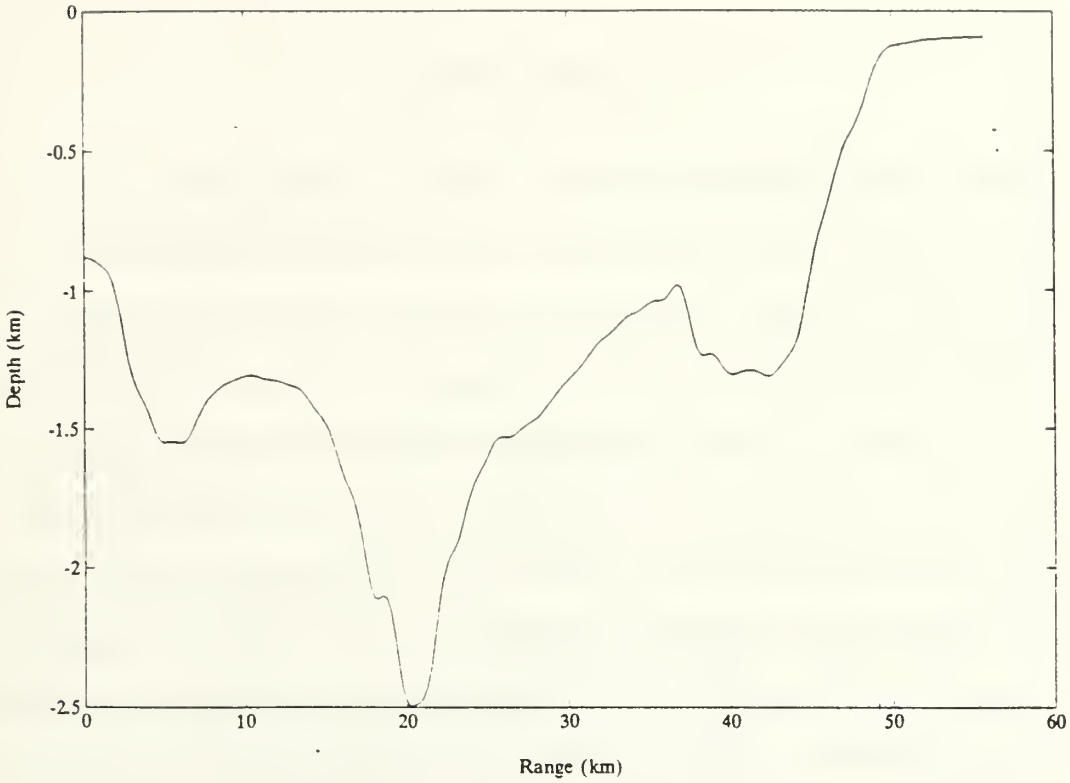

Figure 13. Bathymetry from the source to Station J.

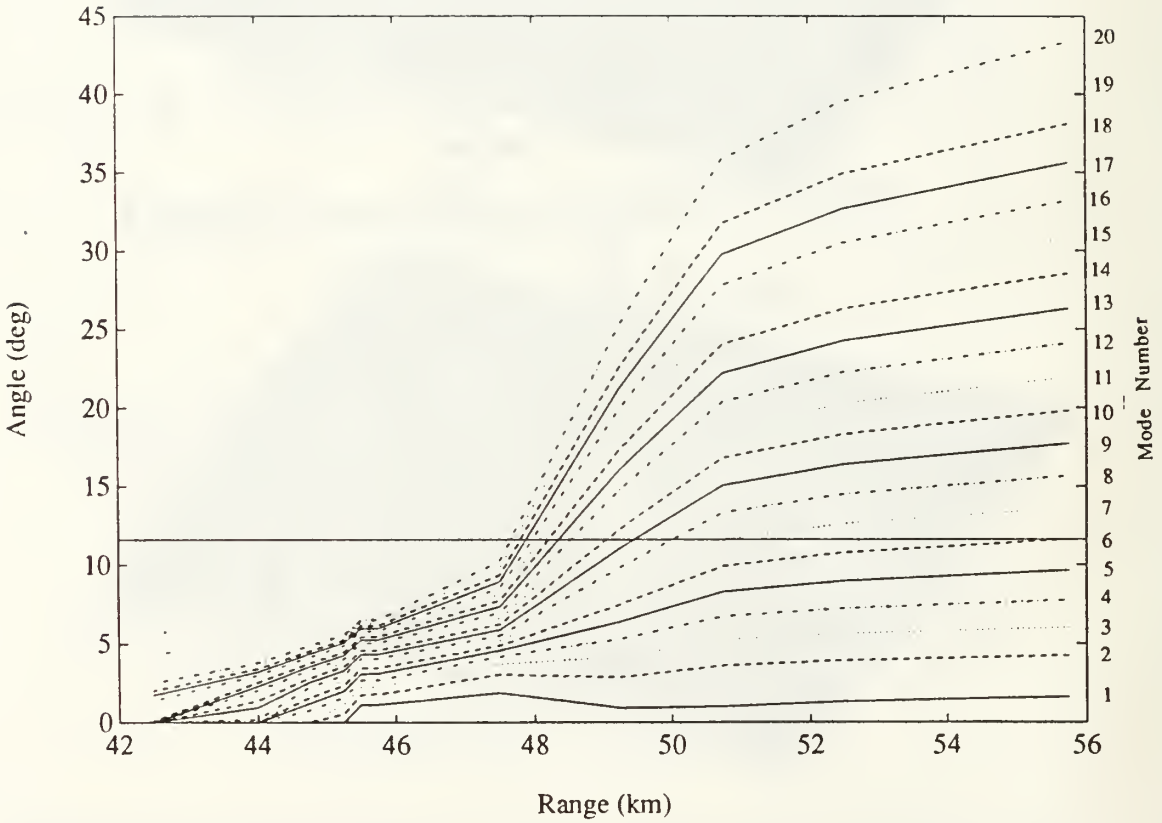

Figure 14. Equivalent-ray angles as a function of mode number and range.

V. CONCLUSIONS

Fourier synthesis using the Collins-Westwood parabolic equation model is effective in modeling short-duration time domain signals. Time domain parabolic equation models can be used effectively in acoustically complex areas, such as Monterey Canyon. Modeling propagation in areas with steep slopes require a method which includes higher order terms and which conserves energy.

Model output from the Fourier synthesis parabolic equation model may be decomposed into normal modes. This provides a tool for understanding acoustic sound transmission. The use of a multiple hydrophone array should allow identification of individual modal sound arrivals, thereby going a long way toward solving the forward problem for acoustic tomography in shallow water.

REFERENCES

[1]J. H. Miller, J. F. Lynch, C.-S. Chiu, E. L. Westreich, J. S. Gerber, R. H. Hippenstiel and E. Chaulk, "Acoustic Measurements of the Surface Wave Spectra in Monterey, Bay using Mode Travel Time Fluctuations," Unpublished Manuscript (1991).

[2]R. C. Dees, "Signal Processing and Preliminary Results in the 1988 Monterey Bay Tomography Experiment," MS Thesis, Naval Postgraduate School, Monterey, CA,1989.

[3]D. F. Smith,"Acoustic Modeling of the Monterey Bay Tomography Experiment,," MS Thesis, Naval Postgraduate School, Monterey, CA,1990.

[4]J. H. Miller, "Estimation of Sea Surface Wave Spectra Using Acoustic Tomography," Doctoral Dissertation, Woods Hole Oceanographic Institution, 1987.

[5]W. Munk and C. Wunsch, "Ocean Acoustic Tomography: A Scheme for Large Scale Monitoring," Deep-Sea Research **26A**, 123-161 (1979).

[6]The Ocean Tomography Group, "A Demonstration of Ocean Acoustic Tomography," Nature **299**(5879),121-125 (1982).

[7]B. Cornnuelle, C. Wunsch, D. Behringer, T. Birdsall, M. Brown, R. Heinmiller, R. Knox, K. Metzger, W. Munk, J. Speisberger, R. Spindel, D. Webb, and P. Worcester, "Tomographic Maps of the Ocean Mesoscale. Part I: Pure Acoustics," J. Phys. Oceanogr. **15**(2),133-152 (1982).

[8]H. A. DeFerrari and H.B. Nguyen, "Acoustic reciprocal transmission experiments, Florida Straits," J. Acoust. Soc. Am. **79**,299-315 (1986).

[9]M. D. Collins and E. K. Westwood, "A higher-order energy conserving parabolic equation for range dependent ocean depth, sound speed, and density," J. Acoust. Soc. Am. **89**, 1068-1075 (1991).

[10]M. D. Collins, "Benchmark calculations for higher-order parabolic equations," J. Acoust. Soc. Am. **87**, 1535-1538 (1990).

[11]M. D. Collins, "FEPE user's guide," NORDA Tech Note 365 (NORDA, Stennis Space Center, MS 39529, 1988).

[12]M. D. Collins, "A higher order parabolic equation for wave propagation in an ocean overlying an elastic bottom," J. Acoust. Soc. Am. **86**, 1459-1464 (1989).

[13]M. D. Collins, "Higher order Padé approximations for accurate and stable elastic parabolic equations with application to interface wave propagation," J. Acoust. Soc. Am **89**, 1050-1057 (1991).

[14]L. J. Ziomek, *A Linear Systems Theory Approach*, (Academic Press Inc, Orlando, 1985), p. 7.

[15]R. B. Evans and K. E. Gilbert, "Acoustic Propagation in a Refracting Ocean Waveguide with an Irregular Interface,"Comp. and Maths. with Appls.**2** (7/8), 795-805 (1985).

[16]C.-S. Chiu and L. L. Ehret, "Computation of Sound Propagation in a Three-dimensionally Varying Ocean: A Coupled Normal Mode Approach," *Computational Acoustics - Volume 1*, (North-Holland, 1990), p 187-202.

[17]D. F. St. Mary, D. Lee, and G. Botseas, "A Modified Wide Angle Wave Equation," J. Comput. Phys. **71**, 305-315 (1987).

[18]D. Lee and S. T. McDaniel, "Ocean Acoustic Propagation by Finite Difference Methods," Comput. Math. Applic. **14**(5),305-423 (1987).

[19]National Oceanic and Atmospheric Administration, "Documentation for Dissemination of NOS/NOAA Gridded EEZ Bathymetric Data," Ocean Mapping Section, N/CG224, NOAA Rockville Maryland.

[20]C. S. Clay and H. Medwin, *Acoustical Oceanography* (J. Wiley and Sons, New York, 1977), p. 258, 306.

[21]C. T. Tindle and K. M. Guthrie, "Rays as Interfering Modes in Underwater Acoustics," J. Sound and Vibration **34**(2), 291-295 (1974).

[22]K. M. Guthrie and C. T. Tindle, "Ray Effects in the Normal Mode Approach to Underwater Acoustics," J. Sound and Vibration **47**(3), 403-413 (1976).

INITIAL DISTRIBUTION LIST

		No. Copies
1.	Defense Technical Information Center Cameron Station Alexandria, VA 22304-6145	2
2.	Library, Code 0142 Naval Postgraduate School Monterey, CA 93943-5100	2
3.	Prof. Ching-Sang Chiu, Code 68Ci Department of Oceanography Naval Postgraduate School Monterey, CA 93943-5100	2
4.	Prof. James H. Miller, Code 62Mr Department of Electrical and Computer Engineering Naval Postgraduate School Monterey, CA 93943-5100	2
5.	Dr. Thomas Kinder Coastal Oceanography Program Office of Naval Research Arlington, VA 22217	1
6.	Library Scripps Institution of Oceanography University of California, San Diego La Jolla, CA	1
7.	Chairman, Department of Oceanography Code OC/Co Naval Postgraduate School Monterey, CA 93943-5100	1
8.	Library Naval Oceanography Office Stennis Space Center, MS	1

9. Oceanography of the Navy, OP 095 — 1
Pentagon
Washington, D. C. 20350-2000

10. Eric Westreich — 2
1225 Vanderbilt Way
Sacramento, CA 95825